

PERFORMANCE ANALYSIS OF GENERAL PILOT-AIDED LINEAR CHANNEL ESTIMATION IN LTE OFDMA SYSTEMS WITH APPLICATION TO SIMPLIFIED MMSE SCHEMES

Samir Omar, Andrea Ancora

NXP Semiconductors
Business Line Cellular Systems
505 route des Lucioles
06560 Sophia Antipolis, France
{samir.omar, andrea.ancora}@nxp.com

Dirk T.M. Slock

EURECOM Institute
Mobile Communications Dept.
2229 route des Crêtes, BP 193
06904 Sophia Antipolis Cedex, France
dirk.slock@eurecom.fr

ABSTRACT

In this paper we provide a general framework for the performance analysis of pilot-aided linear channel estimators class including the general interpolation, Least Squares (LS), *regularized* LS, Minimum-Mean-Squared-Error (MMSE) and approximated MMSE estimators. The analysis is performed from the perspective of Long Term Evolution Orthogonal Frequency Division Multiple Access (LTE OFDMA) down-link systems. We also propose two novel modified MMSE schemes, an Exponential Mismatched MMSE and a Simplified MMSE, to overcome the high implementation complexity of the MMSE and offering improvements to other known approximated methods. At the end, we verify the analytical results by means of Monte-Carlo simulations in terms of Normalized Mean Square Error (NMSE) and coded Bit Error Rate (BER).

Index Terms— OFDMA, channel estimation, interpolation, Least-Squares, Minimum-Mean-Squared-Error

1. INTRODUCTION AND SYSTEM DEFINITION

In December 2004, the Third Generation Partnership Program (3GPP) members started a feasibility study on the enhancement of the Universal Terrestrial Radio Access (UTRA) in the aim of continuing the long time frame competitiveness of the 3G UMTS technology beyond HSPA (High Speed Packet Access). This project was called Evolved-UTRAN or Long Term Evolution (LTE).

Orthogonal Frequency Division Multiple Access (OFDMA) was chosen as a multiple-access scheme for the Frequency Domain Duplexing Down-Link (FDD DL) transmission [1]. The discrete-time OFDMA transceiver model is schematically depicted in figure 2. The users' complex constellation symbols are mapped on $K - 1$ occupied sub-carriers spaced by $\Delta f_{sc} = 15$ kHz and padded with zeros on the DC and band-edges sub-carriers (where these last ones can be considered as a guard-band) to fit the Inverse Fast Fourier Transform (IFFT)

of order N . The resulting sequence of length N is cyclic-prefixed by L_{CP} samples. The Cyclic-Prefix (CP) length L_{CP} is variable and configured by the system to be longer than the channel delay spread L . In LTE, two cyclic-prefixes are considered allowing flexible system deployment (small and large cell radius): a short one of duration $4.7 \mu s$ and a long one of $16.7 \mu s$. The sequence of $N + L_{CP}$ samples $s(k)$ is convolved with a discrete time Finite Impulse Response (FIR) channel (eventually time varying but assumed constant over one OFDMA symbol) modeling the wireless channel at a sampling rate $T_s = 1/(N\Delta f_{sc})$. At the User Equipment (UE) side, the received sequence $r(k)$ results from the channel output signal added with complex circular white Gaussian noise $w(k)$. Assuming perfect synchronization, the CP samples are discarded and the remaining N samples are FFT processed to retrieve the complex constellation symbols transmitted over the orthogonal sub-channels. The system bandwidth is scalable by controlling the IFFT/FFT size N of the OFDMA symbol and keeping the sub-carrier spacing constant: table 1 resumes the main system transmission parameters considered for LTE. With a FFT size varying from 128 to 2048, the supported DL band-width ranges from 1.25 MHz to 20 MHz. Figure 2 represents, without loss of generality, one possible FDD LTE slot structure, namely the short-prefixed case composed of 7 OFDMA symbols. The slot structure embeds pilot symbols, also referred to as Reference Signal (RS), used to estimate the channel at the receiver side. The channel estimation is needed for channel equalization and general link quality measurements. These pilot symbols are interleaved with the data symbols in the frequency domain and are disposed on a uniform grid occupying the first and the fifth OFDMA symbols of each slot and placed every $M = 6$ sub-carriers.

2. PILOT-AIDED LINEAR CHANNEL ESTIMATION

Although the general channel estimation problem in case of single antenna transmissions is two-dimensional [2], i.e. is to

be carried jointly in the frequency and time domains, it is normally separated into two one-dimensional estimation steps [3] for ease of implementation. In this context, we deal in particular with the channel estimation problem over one OFDMA symbol (specifically the symbol containing the RS) to exploit the frequency domain characteristics and instead we do not consider its time-varying characteristics due to Doppler effect in the aim of exploiting correlation in time.

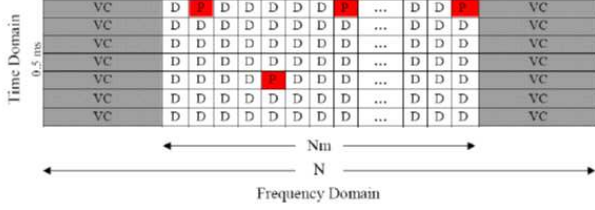


Fig. 1. LTE OFDMA slot structure.

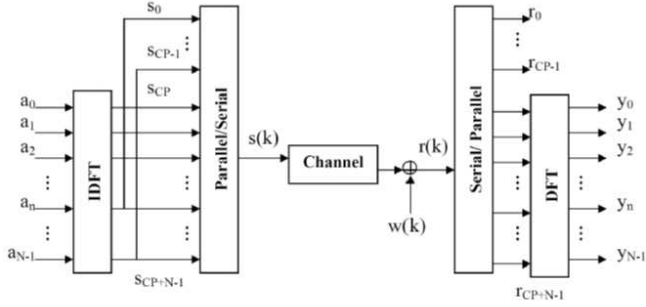


Fig. 2. LTE OFDMA transceiver.

In the OFDMA LTE context, as for any comb-distributed pilot OFDM system [4], the Channel Transfer Function (CTF) is ML estimated in the frequency domain at the pilot positions by de-correlating the constant modulus Reference Signal pilot sequence. Using matrix notation, it can be modeled as:

$$\hat{\mathbf{H}}_p = \mathbf{H}_p + \tilde{\mathbf{H}}_p = \mathbf{F}_p \mathbf{h} + \tilde{\mathbf{H}}_p \quad (1)$$

where

- $P = \lceil K/M \rceil$ is the number of available pilots where K is the number of occupied sub-carriers (including DC).
- \mathbf{h} is the $L \times 1$ Channel Impulse Response (CIR) vector. The effective channel length $L \leq L_{CP}$ is assumed to be known.
- \mathbf{F}_p is the $P \times L$ matrix obtained by selecting the rows corresponding to the pilot positions and the first L columns of the $N \times N$ Discrete Fourier Transform (DFT) matrix whose elements are $(\mathbf{F})_{n,k} = e^{-\frac{j2\pi}{N}(nk)}$ with $0 \leq n \leq N-1$ and $0 \leq k \leq N-1$;

- $\tilde{\mathbf{H}}_p$ is the $P \times 1$ zero-mean complex circular white noise vector whose $L \times L$ covariance matrix is $\mathbf{C}_{\tilde{\mathbf{H}}_p} = \sigma_{\tilde{\mathbf{H}}_p}^2 \mathbf{I}_L$;

2.1. Channel Estimation by interpolation

2.1.1. Linear interpolation estimator

The natural approach to estimate the whole CTF is to interpolate the CTF estimate on pilot positions $\hat{\mathbf{H}}_p$. In the general case, let \mathbf{A} be a generic interpolation filter and the interpolated CTF estimate can be written as:

$$\hat{\mathbf{H}}_i = \mathbf{A} \hat{\mathbf{H}}_p \quad (2)$$

Substituting (1) in (2), the error of the interpolated CTF estimate is:

$$\tilde{\mathbf{H}}_i = \mathbf{H} - \hat{\mathbf{H}}_i = (\mathbf{F}_L - \mathbf{A}\mathbf{F}_p) \mathbf{h} - \mathbf{A}\tilde{\mathbf{H}}_p \quad (3)$$

where $\mathbf{H} = \mathbf{F}_L \mathbf{h}$ and \mathbf{F}_L is the $N \times L$ matrix obtained taking the first L columns of the Fourier transform matrix.

The error covariance matrix is:

$$\mathbf{C}_{\tilde{\mathbf{H}}_i} = (\mathbf{F}_L - \mathbf{A}\mathbf{F}_p) \mathbf{C}_h (\mathbf{F}_L - \mathbf{A}\mathbf{F}_p)^H + \sigma_{\tilde{\mathbf{H}}_p}^2 \mathbf{A}\mathbf{A}^H \quad (4)$$

being $\mathbf{C}_h = \mathbf{E}\mathbf{h}\mathbf{h}^H$ the channel covariance matrix, $\{\cdot\}^H$ and $\mathbf{E}\{\cdot\}$ denoting, respectively, the Hermitian and the expectation operators.

Although pulse-shaping is not mandated in LTE, receiver front-end consists of an anti-aliasing low-pass filtering.

Therefore the channel and its covariance matrix can effectively be modeled as:

$$\mathbf{h} = \mathbf{P}\mathbf{u} \quad \text{and} \quad \mathbf{C}_h = \mathbf{P}\mathbf{C}_u\mathbf{P}^H \quad (5)$$

where \mathbf{P} is the matrix of the equivalent pulse-shaping filter, \mathbf{u} is the discrete-time uncorrelated multipath fading channel vector and

$$\mathbf{C}_u = \mathbf{E}\mathbf{u}\mathbf{u}^H = \text{diag} \left(\sigma_{u_0}^2, \sigma_{u_1}^2, \dots, \sigma_{u_{L_{MP}-1}}^2 \right)$$

is its diagonal covariance matrix normally assimilated to the channel Power Delay Profile (PDP).

Recalling equation (2), the first intuitive move is to use linear interpolation. Although the straightforward filter structure \mathbf{A} is not described, a little bit investigation of (2) reveals that the linear interpolation estimator is biased from the deterministic viewpoint while it is unbiased from the Bayesian viewpoint regardless of the structure of \mathbf{A} .

2.1.2. IFFT estimator

The second natural approach to retrieve the whole CTF estimate is by IFFT interpolation. The IFFT CTF estimate interpolated over all sub-carriers can be obtained by using in (2):

$$\mathbf{A} = \frac{1}{P} \mathbf{F}_L \mathbf{F}_p^H \quad (6)$$

Slot duration [ms]	0.5					
Sub-carrier spacing Δf_{sc} [kHz]	15					
Transmission BW [MHz]	1.25	2.5	5	10	15	20
Sampling frequency [MHz]	1.92	3.84	7.68	15.36	23.04	30.72
FFT size N	128	256	512	1024	1536	2048
Occupied sub-carriers (including DC) K	76	151	301	601	901	1201

Table 1. LTE OFDMA parameters.

Hence, the *IFFT* estimator is given by:

$$\hat{\mathbf{H}}_{\text{IFFT}} = \frac{1}{P} \mathbf{F}_L \mathbf{F}_p^H \hat{\mathbf{H}}_p \quad (7)$$

The *IFFT* interpolated CTF estimate error and its covariance matrix, applying (1) and (6) into (2), becomes:

$$\tilde{\mathbf{H}}_{\text{IFFT}} = \mathbf{F}_L \left(\mathbf{I}_L - \frac{1}{P} \mathbf{F}_p^H \mathbf{F}_p \right) \mathbf{h} - \frac{1}{P} \mathbf{F}_L \mathbf{F}_p^H \tilde{\mathbf{H}}_p \quad (8)$$

$$\mathbf{C}_{\tilde{\mathbf{H}}_{\text{IFFT}}} = \left(\mathbf{F}_L - \frac{1}{P} \mathbf{F}_L \mathbf{F}_p^H \mathbf{F}_p \right) \mathbf{C}_h \quad (9)$$

$$\left(\mathbf{F}_L - \frac{1}{P} \mathbf{F}_L \mathbf{F}_p^H \mathbf{F}_p \right)^H + \frac{1}{P^2} \sigma_{\tilde{\mathbf{H}}_p}^2 \mathbf{F}_L \mathbf{F}_p^H \mathbf{F}_p \mathbf{F}_L^H$$

In the approximation of $\mathbf{I}_L \approx \frac{1}{P} \mathbf{F}_p^H \mathbf{F}_p$, the estimator would be unbiased and its error covariance matrix would reduce to:

$$\mathbf{C}_{\tilde{\mathbf{H}}_{\text{IFFT}}} \approx \frac{1}{P} \sigma_{\tilde{\mathbf{H}}_p}^2 \mathbf{F}_L \mathbf{F}_L^H \quad (10)$$

Given the LTE system parameters and the pilot structure, in practice, $\frac{1}{P} \mathbf{F}_p^H \mathbf{F}_p$ is far from being a multiple of an identity matrix: the approximation would be an equality when $K = N, N/M > L$ and N/M being an integer, i.e. the system should be dimensioned without guard-bands and the pilot should be disposed with a spacing which is dividing exactly the FFT order N, namely a power of two. Therefore, according to (8), the estimator $\hat{\mathbf{H}}_{\text{IFFT}}$ is biased as for the linear interpolation case if the channel is deterministic and unbiased from the Bayesian point of view.

We remand to the simulation results section of this paper for a comparison of their respective performances.

2.2. General approach to linear channel estimation

Compared to the simple approaches presented in the previous section, more elaborated linear estimators derived from both deterministic and statistical viewpoint proposed in [5], [6] and [7], namely LS, Regularized LS, MMSE and Mismatched MMSE in addition to the novel estimators presented in the following sections, can all be expressed under the general formulation:

$$\hat{\mathbf{H}}_{\text{gen}} = \mathbf{B} (\mathbf{G}^H \mathbf{G} + \mathbf{R})^{-1} \mathbf{G}^H \hat{\mathbf{H}}_p \quad (11)$$

Where \mathbf{B} , \mathbf{G} and \mathbf{R} are matrices that vary according to each estimator as detailed in the following. With (1) and (11),

we obtain the error expression:

$$\tilde{\mathbf{H}}_{\text{gen}} = \left(\mathbf{F}_L - \mathbf{B} (\mathbf{G}^H \mathbf{G} + \mathbf{R})^{-1} \mathbf{G}^H \mathbf{F}_p \right) \mathbf{h} + \quad (12)$$

$$- \mathbf{B} (\mathbf{G}^H \mathbf{G} + \mathbf{R})^{-1} \mathbf{G}^H \tilde{\mathbf{H}}_p$$

and its covariance matrix:

$$\mathbf{C}_{\tilde{\mathbf{H}}_{\text{gen}}} = \left(\mathbf{F}_L - \mathbf{B} (\mathbf{G}^H \mathbf{G} + \mathbf{R})^{-1} \mathbf{G}^H \mathbf{F}_p \right) \mathbf{C}_h \quad (13)$$

$$\left(\mathbf{F}_L - \mathbf{B} (\mathbf{G}^H \mathbf{G} + \mathbf{R})^{-1} \mathbf{G}^H \mathbf{F}_p \right)^H +$$

$$+ \sigma_{\tilde{\mathbf{H}}_p}^2 \mathbf{B} (\mathbf{G}^H \mathbf{G} + \mathbf{R})^{-1} \mathbf{G}^H \mathbf{G} (\mathbf{G}^H \mathbf{G} + \mathbf{R})^{-1} \mathbf{B}^H$$

2.2.1. LS estimator

The LS estimator discussed in [5] can be inferred by choosing:

$$\mathbf{B} = \mathbf{F}_L, \mathbf{G} = \mathbf{F}_p \text{ and } \mathbf{R} = \mathbf{0}_L \quad (14)$$

with $\mathbf{0}_L$ being the $L \times L$ matrix containing zeros. And the estimator appears as:

$$\hat{\mathbf{H}}_{\text{LS}} = \mathbf{F}_L (\mathbf{F}_p^H \mathbf{F}_p)^{-1} \mathbf{F}_p^H \hat{\mathbf{H}}_p \quad (15)$$

Substituting (1) and (14) in (12) and (13), the error reduces to:

$$\tilde{\mathbf{H}}_{\text{LS}} = -\mathbf{F}_L (\mathbf{F}_p^H \mathbf{F}_p)^{-1} \mathbf{F}_p^H \tilde{\mathbf{H}}_p \quad (16)$$

showing that the LS estimator, at least theoretically, is unbiased. Thus, compared to the linear interpolation estimator given by (2), the LS estimator is considered as the perfect interpolator as it sets to zero the bias term of expression (3) with $\mathbf{A} = \mathbf{F}_L (\mathbf{F}_p^H \mathbf{F}_p)^{-1} \mathbf{F}_p^H$. Consequently, the error covariance matrix can be shown to be:

$$\mathbf{C}_{\tilde{\mathbf{H}}_{\text{LS}}} = \sigma_{\tilde{\mathbf{H}}_p}^2 \mathbf{F}_L (\mathbf{F}_p^H \mathbf{F}_p)^{-1} \mathbf{F}_L^H \quad (17)$$

2.2.2. Regularized LS estimator

As evidenced in [7], the LTE system parameters make the LS estimator inapplicable: the expression $(\mathbf{F}_p^H \mathbf{F}_p)^{-1}$ is ill-conditioned due to the large unused portion of the spectrum corresponding to the unmodulated sub-carriers.

To counter this problem, the robust *regularized* LS estimator was used to yield a better conditioning of the matrix

to be inverted by using the same \mathbf{B} and \mathbf{G} as for the LS estimator but introducing the regularization matrix $\mathbf{R} = \alpha \mathbf{I}_L$ with α being a constant (off-line) chosen to optimize the performance of the estimator in a given Signal-to-Noise Ratio (SNR) working range.

Hence, we can write the estimator as follows:

$$\hat{\mathbf{H}}_{\text{reg,LS}} = \mathbf{F}_L \left(\mathbf{F}_p^H \mathbf{F}_p + \alpha \mathbf{I}_L \right)^{-1} \mathbf{F}_p^H \hat{\mathbf{H}}_p \quad (18)$$

The expressions for the error and the error covariance matrix of this estimator can be deduced directly from (12) and (13) by substituting \mathbf{B} , \mathbf{G} and \mathbf{R} with their corresponding expressions.

2.2.3. MMSE estimator

Using equations (11), (12) and (13), we can formulate the MMSE estimator [5] by denoting:

$$\mathbf{B} = \mathbf{F}_L, \mathbf{G} = \mathbf{F}_p \text{ and } \mathbf{R} = \sigma_{\tilde{\mathbf{H}}_p}^2 \mathbf{C}_h^{-1} \quad (19)$$

thus giving

$$\hat{\mathbf{H}}_{\text{MMSE}} = \mathbf{F}_L \left(\mathbf{F}_p^H \mathbf{F}_p + \sigma_{\tilde{\mathbf{H}}_p}^2 \mathbf{C}_h^{-1} \right)^{-1} \mathbf{F}_p^H \hat{\mathbf{H}}_p \quad (20)$$

Again, applying (1) and (19) in (12) and (13), the error of the MMSE estimator is:

$$\begin{aligned} \tilde{\mathbf{H}}_{\text{MMSE}} = & \mathbf{F}_L \left(\mathbf{I}_L - \left(\mathbf{F}_p^H \mathbf{F}_p + \sigma_{\tilde{\mathbf{H}}_p}^2 \mathbf{C}_h^{-1} \right)^{-1} \mathbf{F}_p^H \mathbf{F}_p \right) \mathbf{h} + \\ & - \mathbf{F}_L \left(\mathbf{F}_p^H \mathbf{F}_p + \sigma_{\tilde{\mathbf{H}}_p}^2 \mathbf{C}_h^{-1} \right)^{-1} \mathbf{F}_p^H \tilde{\mathbf{H}}_p \end{aligned} \quad (21)$$

and the error covariance matrix:

$$\begin{aligned} \mathbf{C}_{\tilde{\mathbf{H}}_{\text{MMSE}}} = & \mathbf{F}_L \left(\mathbf{I}_L - \left(\mathbf{F}_p^H \mathbf{F}_p + \sigma_{\tilde{\mathbf{H}}_p}^2 \mathbf{C}_h^{-1} \right)^{-1} \mathbf{F}_p^H \mathbf{F}_p \right) \\ & \mathbf{C}_h \left(\mathbf{I}_L - \left(\mathbf{F}_p^H \mathbf{F}_p + \sigma_{\tilde{\mathbf{H}}_p}^2 \mathbf{C}_h^{-1} \right)^{-1} \mathbf{F}_p^H \mathbf{F}_p \right)^H \mathbf{F}_L^H + \\ & + \sigma_{\tilde{\mathbf{H}}_p}^2 \mathbf{F}_L \left(\mathbf{F}_p^H \mathbf{F}_p + \sigma_{\tilde{\mathbf{H}}_p}^2 \mathbf{C}_h^{-1} \right)^{-1} \mathbf{F}_p^H \mathbf{F}_p \\ & \left(\mathbf{F}_p^H \mathbf{F}_p + \sigma_{\tilde{\mathbf{H}}_p}^2 \mathbf{C}_h^{-1} \right)^{-1} \mathbf{F}_L^H \end{aligned} \quad (22)$$

2.2.4. Mismatched MMSE estimator

To avoid the estimation of the second order channel statistics \mathbf{C}_h and of the consequent on-line inversion of a $L \times L$ matrix required in the straightforward application of the MMSE of (20), the channel PDP can be assumed uniform [6]. Hence, in this *Mismatched*-MMSE formulation, \mathbf{C}_h is imposed to have the structure of an identity matrix.

With reference to the general formulation in (11), this scheme consists in taking the same \mathbf{B} and \mathbf{G} of (19) but defining $\mathbf{R} = \sigma_{\tilde{\mathbf{H}}_p}^2 / \sigma_h^2 \cdot \mathbf{I}_L$ to give the expression

$$\hat{\mathbf{H}}_{\text{M-MMSE}} = \mathbf{F}_L \left(\mathbf{F}_p^H \mathbf{F}_p + \sigma_{\tilde{\mathbf{H}}_p}^2 / \sigma_h^2 \cdot \mathbf{I}_L \right)^{-1} \mathbf{F}_p^H \hat{\mathbf{H}}_p \quad (23)$$

Interestingly, we notice that this estimator is in practice equivalent to *regularized* LS estimator in 2.2.2. where the only difference lies in the fact that the ratio $\sigma_{\tilde{\mathbf{H}}_p}^2 / \sigma_h^2$ can be estimated and therefore adapted.

For a given channel length L , to avoid the on-line inversion of the matrix $\left(\mathbf{F}_p^H \mathbf{F}_p + \sigma_{\tilde{\mathbf{H}}_p}^2 / \sigma_h^2 \cdot \mathbf{I}_L \right)$, the practical approach would consist in dividing the SNR working range into sub-ranges and storing different versions of the matrix inverted off-line for each sub-range.

2.2.5. Exponential mismatched MMSE estimator

Realistic channel PDP are likely exponentially decaying rather than uniform as assumed by the *mismatched*-MMSE discussed above. We therefore propose an *exponential mismatched*-MMSE estimator that approximates \mathbf{C}_h by a diagonal matrix whose entries are decaying exponentially. This is done by using (19) and taking:

$$\mathbf{R} = \frac{\sigma_{\tilde{\mathbf{H}}_p}^2}{\sigma_h^2} \mathbf{C}_{L,\text{exp}}^{-1} \text{ and } \mathbf{C}_{L,\text{exp}} = \gamma \cdot \text{diag} \left(e^{-n \frac{\ln(2L)}{L}} \right) \quad (24)$$

with $0 \leq n \leq L - 1$ and $\gamma = 1 / \sum_{n=0}^{L-1} e^{-n \frac{\ln(2L)}{L}}$. Hence, it is represented by:

$$\hat{\mathbf{H}}_{\text{exp-MMSE}} = \mathbf{F}_L \left(\mathbf{F}_p^H \mathbf{F}_p + \frac{\sigma_{\tilde{\mathbf{H}}_p}^2}{\sigma_h^2} \mathbf{C}_{L,\text{exp}}^{-1} \right)^{-1} \mathbf{F}_p^H \hat{\mathbf{H}}_p \quad (25)$$

Again, the error and the error covariance matrix can be deduced from (12) and (13) by substituting \mathbf{B} , \mathbf{G} and \mathbf{R} with their corresponding expressions.

Compared to the uniform channel distribution assumption of *Mismatched*-MMSE, the estimator reveals to be less sensitive to the channel length mis-estimation due to the exponential decaying nature and thus less versions of the inverse of the matrix $\left(\mathbf{F}_p^H \mathbf{F}_p + \frac{\sigma_{\tilde{\mathbf{H}}_p}^2}{\sigma_h^2} \mathbf{C}_{L,\text{exp}}^{-1} \right)$ can be precomputed and stored.

2.2.6. Simplified MMSE estimator

As already mentioned, the direct implementation of the MMSE estimator in (20) requires the solution of two problems:

1. The estimation of the variance of the noise and channel second order statistics;
2. The on-line inversion of the large $L \times L$ matrix

$$\mathbf{S}_{\text{MMSE}} = \mathbf{F}_p^H \mathbf{F}_p + \sigma_{\tilde{\mathbf{H}}_p}^2 \mathbf{C}_h^{-1} \quad (26)$$

whenever the channel and noise statistics change.

Assuming the required estimations available, we propose here an original solution to overcome in particular the second problem. The idea behind our simplified MMSE estimator lies in separating the problem of the approximation of (26) into, first, considering a fixed initialization matrix \mathbf{S}_{init} , as detailed below, and then in enhancing the first approximation by inserting the contribution of a portion of the PDP corresponding to the strongest taps, denoted *captured taps* in the following, on the diagonal of the initialization matrix \mathbf{S}_{init} .

As for previous approximated methods, the dependency from the noise variance can be maintained by quantization of the SNR into sub-ranges and storing a limited set of \mathbf{S}_{init} values.

Let us define:

$$\mathbf{S}_{\text{init}} = \mathbf{F}_p^H \mathbf{F}_p + \sigma_{\mathbf{H}_p}^2 \mathbf{C}_{\text{init}}^{-1} \quad (27)$$

where $\mathbf{C}_{\text{init}} = \beta \mathbf{I}_L$ and β is a constant carefully chosen to provide sufficiently good performance of the estimator.

The matrix \mathbf{S}_{MMSE} can be approximated by:

$$\mathbf{S}_{\text{SMMSE}} = \mathbf{S}_{\text{init}} + \mathbf{D} \Delta \mathbf{S} \mathbf{D}^H \quad (28)$$

where

1. \mathbf{D} is a $L \times M$ selector matrix called after the role it plays in the selection of the positions where the elements of the PDP profile (that correspond to the M captured taps) are going to be located on the diagonal of \mathbf{S}_{init} . The first column of the matrix \mathbf{D} contains one only in the position that corresponds to the index of the first captured tap and zeros everywhere else and the second column contains one only in the position that corresponds to the index of the second captured tap and zeros everywhere else and so on.
2. $\Delta \mathbf{S}$ is a diagonal matrix containing the inverse of the power of the captured taps after removing the effect of initialization, i.e. $\Delta \mathbf{S}_{m,m} = \sigma_{\mathbf{H}_p}^2 (\mathbf{C}_{h_m}^{-1} - \beta^{-1})$ where \mathbf{h}_m is a vector contains the M captured taps.

Applying the *Matrix Inversion Lemma* (MIL), we can write:

$$\mathbf{S}_{\text{SMMSE}}^{-1} = \mathbf{S}_{\text{init}}^{-1} - \mathbf{S}_{\text{init}}^{-1} \mathbf{D} (\mathbf{D}^H \mathbf{S}_{\text{init}}^{-1} \mathbf{D} + \Delta \mathbf{S}^{-1})^{-1} \mathbf{D}^H \mathbf{S}_{\text{init}}^{-1} \quad (29)$$

It is worth mentioning that the number of significant taps in terms of power is usually much less than the overall length of the CIR. Thus, the importance of the proposed estimator stems from the fact that we take advantage of this property to reduce the size of the matrix to be inverted on-line from $L \times L$ to $M \times M$ with $M \ll L$. Another important aspect of the proposed estimator is that the accuracy of the approximation is traded-off with the complexity by controlling the number of captured taps. Therefore, the more the number of the captured

taps the larger the size of the matrix to be inverted on-line and vice versa.

Finally the estimated CTF is given by:

$$\hat{\mathbf{H}}_{\text{SMMSE}} = \mathbf{F}_L \mathbf{S}_{\text{SMMSE}}^{-1} \hat{\mathbf{H}}_p \quad (30)$$

Comparing (30) with (11), the *Simplified* MMSE consists in choosing:

$$\mathbf{B} = \mathbf{F}_L, \mathbf{G} = \mathbf{F}_p \text{ and } \mathbf{R} = \sigma_{\mathbf{H}_p}^2 \mathbf{C}_{\text{init}}^{-1} + \mathbf{D} \Delta \mathbf{S} \mathbf{D}^H \quad (31)$$

The estimation error and the error covariance matrix expression of the proposed estimator can then be obtained by substituting (31) in (12) and (13).

3. SIMULATION RESULTS

We compare the performances of the estimators by mean of *Truncated-Normalized-Mean-Squared-Error* (TNMSE).

For each estimator $\hat{\mathbf{H}}$, the TNMSE is computed from its covariance matrix $\mathbf{C}_{\hat{\mathbf{H}}}$ and the true channel $\mathbf{H} = \mathbf{F}_L \mathbf{h}$ using the following:

$$\text{TNMSE}_{\hat{\mathbf{H}}} = \frac{\text{Tr}(\mathbf{C}_{\hat{\mathbf{H}}})}{\text{Tr}(\mathbf{F}_L \mathbf{C}_h \mathbf{F}_L^H)} \quad (32)$$

where with $\text{Tr}\{\cdot\}$ we denote the truncated trace operator consisting of the *truncated* covariance matrix considering only the K used sub-carriers. For the comparison in figure 3, we used *raised-cosine* pulse-shaping filter with a roll-off factor of $\beta = 0.2$, the SCMA channel and an LTE setup with $N = 1024$ corresponding to the 10 MHz transmission bandwidth case [1]. As for the regularized LS estimator, we use the *regularization* term $\alpha = 0.1$. Connected lines represent the theoretical TNMSE while the dotted points represent the results of simulations. We can first conclude that the *IFFT* and linear interpolation methods yield the lowest performances. Moreover the *regularized* LS and the *mismatched* MMSE prove to perform exactly equally and the TNMSE curve of the latter are therefore omitted in figure 3. The *exponential mismatched-MMSE* and the *simplified* MMSE offer a performance gain over all other sub-optimal estimators but the latter proves to be the one approaching the most the MMSE estimator performance particularly in the low SNR region. To highlight the robustness of our *simplified* MMSE, figure 4 compares its performance to that of the *mismatched-MMSE* where the MMSE is used as a reference. It should be noted that the simulated *mismatched-MMSE* is further approximated by exploiting a limited number of pilots around the sub-carriers to be estimated in order to reduce complexity. It is evident that the performance of *simplified* MMSE exceeds for any SNR that of *mismatched-MMSE* even though only 11 out of 50 taps are captured. Figure 5 compares the performances of the *mismatched-MMSE* and of the *simplified* MMSE in terms of Bit Error Rate with 1/3 Turbo Coding with Block Length

= 4992 bits with Maximum Ratio Combining receiver for QPSK modulation. The decoding performance with *simplified* MMSE channel estimation outperforms that of the *mismatched*-MMSE by 2 dB for BER lower than 10^{-2} .

4. CONCLUSIONS

We have presented a framework allowing the performance analysis of the class of the pilot-aided linear channel estimators in the context of LTE OFDMA systems. Together with the analysis of the impact of LTE system parameters, we proved that the well known *mismatched* MMSE estimator is nothing but the deterministic *regularized* LS estimator. The analysis also showed that there is a large performance gap between the *mismatched* MMSE and the MMSE since the statistical properties of the channel, namely the frequency correlation, are not exploited. To fill this gap, we have proposed two modified versions of the MMSE, namely the exponential mismatched MMSE and the simplified MMSE, aiming at reducing the complexity of the MMSE without sacrificing the performance. This is especially achieved by the latter which shows a great flexibility in trading off the complexity and the performance yielding the closest results to the MMSE.

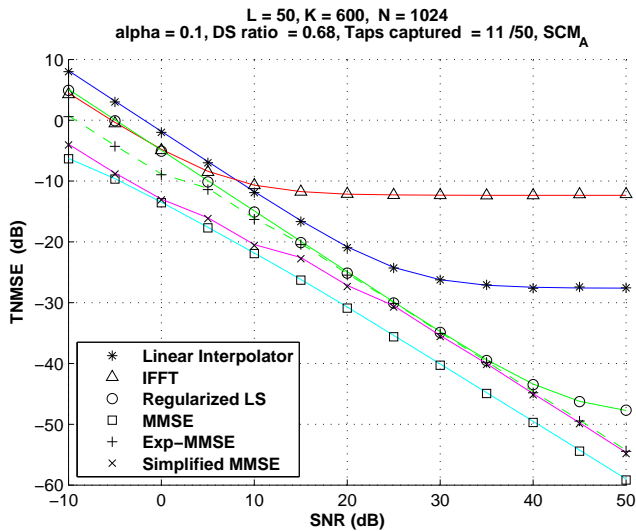


Fig. 3. CTF TNMSE vs. SNR.

5. REFERENCES

- [1] 3GPP WG1, "Ts 36.211: Physical channels and modulation v. 2.0 (rel. 8)," www.3gpp.org, 2007.
- [2] Ye Li et al., "Robust channel estimation for ofdm systems with rapid dispersive fading channels," *IEEE transactions on communications*, vol. 46, pp. 903–912, Jul 1998.
- [3] Frieder Sanzi et al., "An adaptive two-dimensional channel estimator for wireless ofdm with application to mobile dvb-t," *IEEE transactions on broadcasting*, vol. 46, pp. 128–133, Jun 2000.

- [4] J.-J. van de Beek et al., "On channel estimation in ofdm systems," *Vehicular Technology Conference*, vol. 2, pp. 815–819, Jul 1995.
- [5] M. Morelli et al., "A comparison of pilot-aided channel estimation methods for ofdm systems," *Signal Processing, IEEE Transactions on*, vol. 49, pp. 3065–3073, December 2001.
- [6] P. Hoher et al., "Pilot-symbol-aided channel estimation in time and frequency," *Proc. Communication Theory Mini-Conf. (CTMC) within IEEE Global Telecommun. Conf. (Globecom 97)*, pp. 90–96, 1997.
- [7] A. Ancora et al., "Down-sampled impulse response least-squares channel estimation for lte ofdma," *Acoustics, Speech and Signal Processing, 2007. ICASSP 2007. IEEE International Conference on*, vol. 3, pp. III–293–III–296, April 2007.

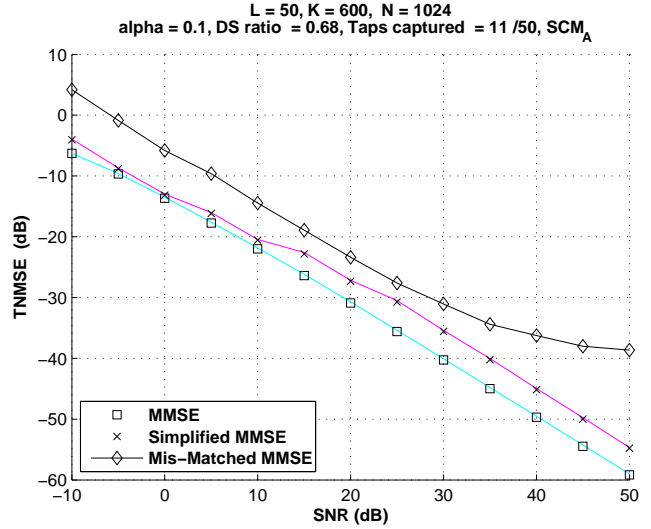


Fig. 4. CTF TNMSE vs. SNR.

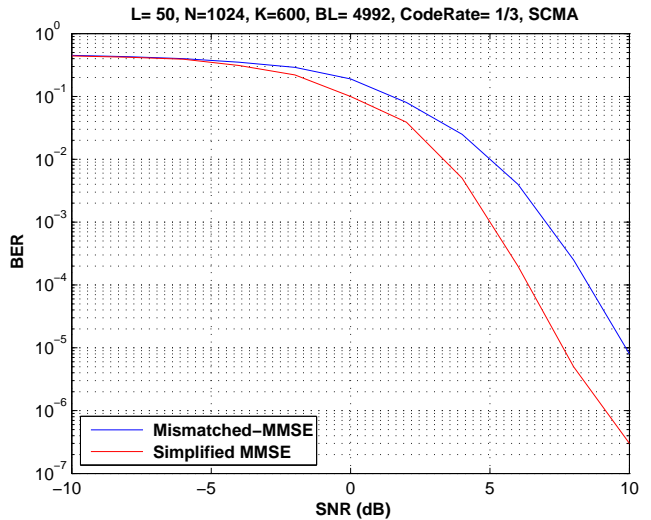


Fig. 5. BER vs. SNR.